



**HAL**  
open science

## The OSCAR V1.4 code: A new dissolution-precipitation model to better simulate the corrosion product transfer in nuclear cooling systems

F. Dacquait, J. Francescato, G. Galassi, F. Broutin, M. Gherrab, D. You, T. Jobert, N. Engler

### ► To cite this version:

F. Dacquait, J. Francescato, G. Galassi, F. Broutin, M. Gherrab, et al.. The OSCAR V1.4 code: A new dissolution-precipitation model to better simulate the corrosion product transfer in nuclear cooling systems. NPC 2018 - International conference on water chemistry in nuclear reactor systems, Sep 2018, San Francisco, United States. cea-02328968

**HAL Id: cea-02328968**

**<https://cea.hal.science/cea-02328968v1>**

Submitted on 25 Feb 2020

**HAL** is a multi-disciplinary open access archive for the deposit and dissemination of scientific research documents, whether they are published or not. The documents may come from teaching and research institutions in France or abroad, or from public or private research centers.

L'archive ouverte pluridisciplinaire **HAL**, est destinée au dépôt et à la diffusion de documents scientifiques de niveau recherche, publiés ou non, émanant des établissements d'enseignement et de recherche français ou étrangers, des laboratoires publics ou privés.

# THE OSCAR V1.4 CODE: A NEW DISSOLUTION-PRECIPITATION MODEL TO BETTER SIMULATE THE CORROSION PRODUCT TRANSFER IN NUCLEAR COOLING SYSTEMS

**F. Dacquait**  
CEA, DEN, F-13108 Saint-Paul Lez Durance, France.  
frederic.dacquait@cea.fr

**J. Francescatto, G. Galassi, F. Broutin, M. Gherrab, D. You**  
CEA, DEN, France.

**T. Jobert**  
EDF, France.

**N. Engler**  
Framatome, France.

## Abstract

Predicting the radioactive contamination of nuclear reactor circuits is a significant challenge for plant designers and operators. To address this challenge, the French strategy has been focusing on performing experiments in test loops, measuring the PWR contamination and developing a simulation code so named OSCAR.

The process governing the contamination by Activated Corrosion Products (ACPs) of a nuclear cooling system involves many different mechanisms that react with each other. One of the most important mechanisms is the dissolution-precipitation mechanism, which governs the behavior of soluble corrosion products and which is related to water chemistry specifications.

The dissolution-precipitation model has been improved in the new version of OSCAR, OSCAR V1.4. Thanks to this improvement and to the OSCAR chemistry module, PHREEQCEA, the OSCAR V1.4 code can reproduce the impacts of pH and of Zn injection on <sup>60</sup>Co contamination highlighted in a laboratory experiment and can better reproduced the volume activity variations during a cold shutdown.

This new version of the OSCAR code is a powerful tool to predict the contamination of nuclear systems and to analyze the corrosion product behaviors in different conditions and thus to provide explanations of these behaviors.

## Introduction

Predicting the radioactive contamination of nuclear reactor circuits is a significant challenge for plant designers and operators. To address this challenge, the French strategy has been focusing on performing experiments in test loops, measuring the PWR contamination and developing a simulation code so named OSCAR (Outil de Simulation de la Contamination en Réacteur – tOol of Simulation of Contamination in Reactor). The OSCAR code has been developed by CEA in collaboration with EDF and Framatome since the 1970's [1] [2] [3]. The OSCAR code is considered to be not only a tool for numerical simulations and predictions of contamination of nuclear cooling systems but also a tool combining and organizing all new knowledge useful to progress in this field.

The process governing the contamination by Activated Corrosion Products (ACPs) of a nuclear cooling system involves many different mechanisms that react with each other including corrosion-release, dissolution-precipitation, erosion, deposition, convection, purification, activation and radioactive decay. One of the most important mechanisms is the dissolution-precipitation mechanism, which governs the behavior of soluble corrosion products and which is related to water chemistry specifications (pH, dissolved hydrogen concentration, zinc injection...).

The dissolution-precipitation model has been improved in the new version of OSCAR, OSCAR V1.4, released at the end of 2017.

After a presentation of the OSCAR V1.4 code, this paper presents the simulation results of a laboratory experiment, of a typical French PWR and of a typical cold shutdown, and their comparison to experimental data.

**Presentation Of The OSCAR V1.4 Code  
Corrosion Product Transfer Modelling**

The OSCAR code modelling is based on a control volume approach; briefly:

- The PWR systems (RCS, CVCS, RHRS...)¹ are discretized into several control volumes or regions (typically around 100 regions) defined according to the geometric, thermal-hydraulic, neutron, material and operating characteristics.
- Six media can be defined in each control volume: metal, inner oxide, outer oxide/deposit, particles, ions and filters (ion exchange resins and particle filter).
- The following elements Ni, Co, Fe, Cr, Mn, Zn, Ag and Zr and their radioisotopes (<sup>58</sup>Co, <sup>60</sup>Co, <sup>59</sup>Fe...) can be taken into account.
- The mass balances are calculated for each isotope (stable and radioactive) of these metallic elements in each medium of each region using the following equation:

$$\frac{\partial m_i}{\partial t} = \sum_{sources} J_{m_i} - \sum_{sinks} J_{m_i} \quad (1)$$

where  $m_i$  is the mass of isotope  $i$  in a given medium [kg],  $t$  the time [s] and  $J_{m_i}$  the mass rate between 2 media or 2 regions or 2 isotopes [kg.s<sup>-1</sup>].

- The transfer mechanisms taken into account are corrosion-release, dissolution, precipitation, erosion, abrasion, deposition, injection, convection, purification, activation and radioactive decay.

**Transfer Mechanisms**

The main mechanisms involved in the corrosion product transfer (corrosion-release, dissolution-precipitation, erosion and deposition) are presented below.

**Corrosion-Release.** Corrosion of the base metal causes the formation of an inner oxide layer (mainly a chromite), of an outer oxide (a ferrite + metal Ni<sup>o</sup> or NiO in general) and a direct ion release into the coolant. The corrosion and release rates [kg.s<sup>-1</sup>] are given by:

$$J_{corrosion}^{elt} = V_{cor} \cdot S_w \cdot \alpha_{met}^{elt} \quad \text{and} \quad J_{release}^{elt} = V_{rel} \cdot S_w \cdot \alpha_{rel}^{elt} \quad (2) \ \& \ (3)$$

where  $V_{cor}$  and  $V_{rel}$  are the surface corrosion and release rates [kg.m<sup>-2</sup>.s<sup>-1</sup>] calculated by an empirical model as a function of chemistry, temperature and material (or by a power law, logarithmic law or constant value per stage),  $S_w$  is the wet surface area [m<sup>2</sup>],  $\alpha_{met}^{elt}$  is the element fraction in the metal and  $\alpha_{rel}^{elt}$  is the element fraction involved in the release.

**Dissolution-Precipitation.** The main improvement of this version of OSCAR is the review of the dissolution-precipitation model [4]. For isotope  $i$  of element  $elt$ , the dissolution-precipitation rate  $J_{dissol/precip}^{ielt}$  [kg.s<sup>-1</sup>], may be written:

$$J_{dissol/precip}^{ielt} = \frac{S_{dissol/precip}}{1/h + 1/V_{dissol}^{elt}} \left( f_{oxide}^{ielt} \cdot C_{eq,oxide}^{elt} - f_{ion}^{ielt} \cdot C^{elt} \right) \quad (4)$$

with  $V_{dissol}^{elt} = \frac{M_{elt} \cdot \sum \alpha_{phasen(elt)} \cdot v_{phasen(elt)} \cdot V_{dissol}^{phasen(elt)}}{C_{eq,oxide}^{elt}}$  the dissolution velocity of element  $elt$  [m.s<sup>-1</sup>]

---

¹ RCS : Reactor Coolant System – CVCS : Chemical and Volume Control System – RHRS : Residual Heat Removal System

and  $V_{dissol}^{phase_n(elt)} = k_n \cdot (10^{-pH})^{\mu_{1,n}} \cdot (p_{H_2})^{\mu_{2,n}} \cdot (p_{O_2})^{\mu_{3,n}}$  the dissolution surface reaction rate of phase  $n$  [mol.m<sup>-2</sup>.s<sup>-1</sup>]

where  $S_{dissol/precip}$  is the dissolution-precipitation surfaces respectively [m<sup>2</sup>],  $h$  is the mass transfer coefficient of ions in the fluid [m.s<sup>-1</sup>],  $f_{oxide}^{ielt}$  and  $f_{ion}^{ielt}$  are the mass fractions of isotope  $i$  of element  $elt$  in the considered oxide (inner oxide, outer oxide or particles) and ions respectively,  $C_{eq,oxide}^{elt}$  is the ion equilibrium concentration of element  $elt$  in the coolant with respect to the considered oxide [kg.m<sup>-3</sup>],  $C^{elt}$  is the ion concentration of element  $elt$  in the bulk coolant [kg.m<sup>-3</sup>],  $M_{elt}$  is the molar mass of element  $elt$  [kg.mol<sup>-1</sup>],  $\alpha_{phase_n(elt)}$  is the proportion of phase  $n$  containing element  $elt$  in oxide,  $v_{phase_n(elt)}$  is the stoichiometric number of element  $elt$  in phase  $n$ ,  $pH$  is the pH calculated at the wall or bulk coolant temperature,  $p_{H_2}$  and  $p_{O_2}$  are the hydrogen and oxygen partial pressures respectively,  $\mu_{i,n}$  is the reaction orders and  $k_n = A_n e^{-Ea_n/RT}$  is the dissolution surface kinetic constant of phase  $n$  [mol.m<sup>-2</sup>.s<sup>-1</sup>] with  $A_n$  the pre-exponential factor [mol.m<sup>-2</sup>.s<sup>-1</sup>],  $Ea_n$  the activation energy [J.mol<sup>-1</sup>],  $R$  the universal molar gas constant (8,314 J.mol<sup>-1</sup>.K<sup>-1</sup>) and  $T$  the wall or bulk coolant temperature [K].

The ion equilibrium concentration of each element  $C_{eq,oxide}^{elt}$ , the oxide speciation  $\alpha_{phase_n(elt)}$ , the pH and the hydrogen and oxygen partial pressures  $p_{H_2}$  and  $p_{O_2}$  are calculated by the OSCAR chemistry module, PHREEQCEA (a version of the PHREEQC code [5] extended to the PWR temperature range) in combination with a thermodynamic database developed by CEA [6]. PHREEQCEA determines the composition of the ideal solid solution (mixed oxides and any pure solid phases possibly in excess) and the ion equilibrium concentration of each element in relation to the chemical conditions (pH, H<sub>2</sub>, O<sub>2</sub>), the wall or bulk coolant temperature and the masses of the metallic elements of the considered oxide (inner oxide, outer oxide or particles) in each control volume.

The dissolution surface kinetic constants of phases, mainly of nickel, ferrites and chromites, are determined by experiments [7] or are calibrated using OSCAR (see section *Calibration-Validation*). Note that the precipitation rate is expressed with the dissolution kinetic constants.

It should also be noted that Eq. (4) enables the precipitation of an isotope even under unsaturated conditions of the element, i.e.  $C_{eq,oxide}^{elt} - C^{elt} > 0$ , when  $f_{oxide}^{ielt} \cdot C_{eq,oxide}^{elt} - f_{ion}^{ielt} \cdot C^{elt} < 0$ . In this case, it corresponds to the isotope exchange.

**Erosion.** Erosion of a deposit results from the coolant friction forces. The erosion rate,  $J_{eros}$  [kg.s<sup>-1</sup>], is given by:

$$J_{Erosion} = \frac{E}{\Psi} \cdot m_{erod} \quad (5)$$

where  $E$  is the erosion coefficient [s<sup>-1</sup>] based on the Cleaver and Yates model [8] and depending on the shear stress at the wall and the dynamic viscosity of the coolant,  $\Psi$  is the erosion resistance [-] and  $m_{erod}$  is the mass of the deposit that can be eroded [kg].

**Deposition.** The particle deposition rate takes into account:

- the turbulent diffusion and the effects of inertia [9],
- the sedimentation for horizontal ducts [10],
- the thermophoresis for temperature gradients between the coolant and the wall [11],
- the boiling deposition [12].

The deposition rate,  $J_{deposition}$  [kg.s<sup>-1</sup>], may be expressed as follows:

$$J_{deposition} = S_{depos} \cdot V_{depos} \cdot C_{part} \quad (6)$$

where  $S_{depos}$  is the deposition surface [m<sup>2</sup>],  $V_{depos}$  is the deposition velocity of particles [m.s<sup>-1</sup>] and  $C_{part}$  is the particle concentration [kg.m<sup>-3</sup>].

### **Calibration-Validation**

The physical models of the transfer mechanisms presented above need to be calibrated. In particular, for the dissolution-precipitation model, the dissolution surface kinetic constants, the activation energies and the reaction orders for the different phases (ferrite, chromite, Ni°...) are scarcely known in PWR conditions. An experiment in the CEA SOZIE loop has allowed us to estimate the dissolution surface kinetic constant of Ni° at 300 °C [13]. About the ferrites and chromites, the dissolution surface kinetic constants and the proton reaction order have been determined by simulating an experiment carried out by Studsvik (see section *Simulation of a Studsvik experiment*). The activation energies and the reaction orders are also based on the simulation of a typical PWR cold shutdown procedure (see section *Simulation of a cold shutdown*). The erosion parameter K has been calibrated on a simulation of a typical PWR in power operation (see section *Simulation of a typical PWR*) and the particle deposition model has been adjusted by simulating an experiment in the CEA CIRENE loop [14].

After the calibration of physical models on experiments and on a typical French PWR, the OSCAR V1.4 code has been validated by simulating the power operation and cold shutdowns of 6 PWRs with different operating and design characteristics (900/1300/1450 MWe PWRs, Inconel 600MA/600TT/690TT SG tubing, Inconel 718/Zry spacer grids, pH<sub>300°C</sub> of 7.0/7.2, different fuel managements ...) [15].

The calibration and the validation of OSCAR can be carried out particularly thanks to an operational experience unique in the world: to date, about 400 EMECC campaigns performed by CEA in 72 different French and foreign PWRs since 1971 [16]. In addition to the  $\gamma$  surface activities measured using the EMECC device [17], the OSCAR results are compared to other on-site measurements: volume activities and chemical element concentrations<sup>2</sup>.

To obtain the OSCAR results, first it is necessary to provide a set of input data by using a graphical user input interface:

- The geometric parameters of each control volume are the hydraulic diameter and the wet surface ;
- The thermal-hydraulic data, which includes the velocity, the flowrate, the bulk and wall temperatures of the coolant ;
- The materials are defined by their density, their composition and their roughness. Any possible surface treatment is taken into account via the experimental corrosion and release rates ;
- As the activation of the corrosion products is directly proportional to the neutron flux, the power fraction is specified in each part of the vessel. The neutron reaction rates, as a function of PWR type, fuel burnup, <sup>235</sup>U enrichment and Pu content, are extracted from a nuclear database interfaced with OSCAR ;
- In terms of operating data, a cycle is defined by its duration, its power history and its concentration levels in boron, lithium, hydrogen and oxygen ;
- The refueling of fuel assemblies at each end of cycle.

The OSCAR results, including masses, activities, dose rates, transfer rates, chemistry parameters (equilibrium concentrations, speciations, pH, partial pressures...) and thermal hydraulic parameters, are plotted thanks to an user-friendly output interface. Some results obtained on the simulation of the Studsvik experiment and on the simulation of a typical PWR are presented in the next section.

## **OSCAR V1.4 Results**

### ***Simulation of a Studsvik experiment***

Studsvik performed experiments to study the impact of different parameters such as pH, Zn, flow velocity and materials on the <sup>60</sup>Co uptake. We have simulated campaign A described in [18] using the OSCAR V1.4 code. The Studsvik experimental loop is discretized in 11 regions, including 6 regions for the test section (see Fig. 1). The

---

<sup>2</sup> On-site dose rate measurements are not considered because not only they reflect the surface and volume activities but also they depend on the measured components and on the ambient dose rates.

variations of the simulated exposure conditions comply with the experimental exposure conditions (see Fig. 2). Zn is injected in Line B from 200 h,  $\text{pH}_{285^\circ\text{C}}$  varies between 6.9 and 7.6, temperature and hydrogen are constant.

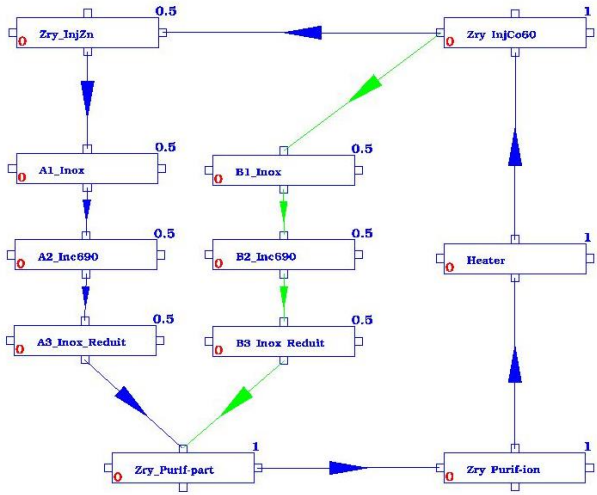


Figure 1: OSCAR V1.4 – Discretization of the Studsvik test loop. Test section: Line A: Zn injection - Line B: No Zn / A1, A3, B1, B3: Stainless Steel - A2, B2: Alloy 690 / A1, A2, B1, B2: Laminar flow - A3, B3: Turbulent flow).

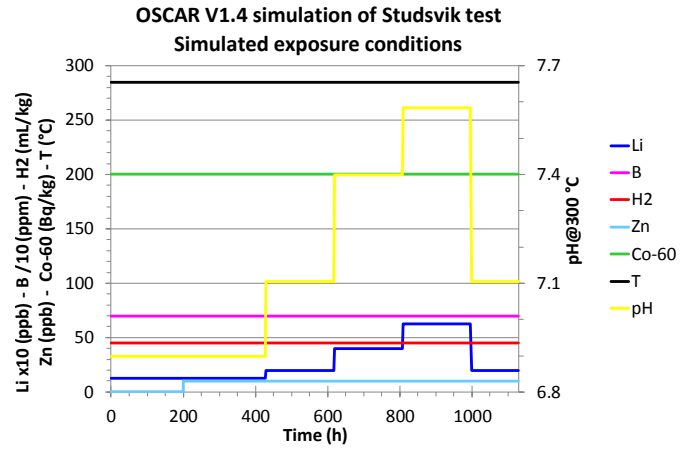


Figure 2: OSCAR V1.4 – Simulated exposure conditions of the Studsvik test.

Fig. 3 illustrates the capacity of OSCAR V1.4 to simulate the effects of pH, zinc, flow velocity and material on  $^{60}\text{Co}$  uptake (on the left the  $^{60}\text{Co}$  activity uptake calculated using OSCAR V1.4, on the right diagram taken from [18]). The  $^{60}\text{Co}$  uptake is higher in turbulent regime (A3 SS section) than in laminar regime (A1 SS section) and for SS (A1 SS section) than for alloy 690 (A2 Alloy 690 section) (laminar regime for both sections). The Zn injection leads to an inflexion in the  $^{60}\text{Co}$  uptake in the 3 sections. Finally, the decrease in pH from 7.6 to 7.1 at the end of the test results in a slight increase in the  $^{60}\text{Co}$  uptake (see red dashed line). All these phenomena are reproduced by OSCAR V1.4, the similarities of variations and levels between the calculation and the measurements are striking. It should be pointed out that few parameters have been adjusted to achieve such a result, mainly the dissolution surface kinetic constant  $k_n$  and the proton reaction order  $\mu_{1,n}$  for ferrites and chromites and on the other hand, the corrosion rate  $V_{cor}$  of SS and alloy 690. A detailed description of the simulation, the values of the parameters, all the OSCAR results and their further analysis are given in [19].

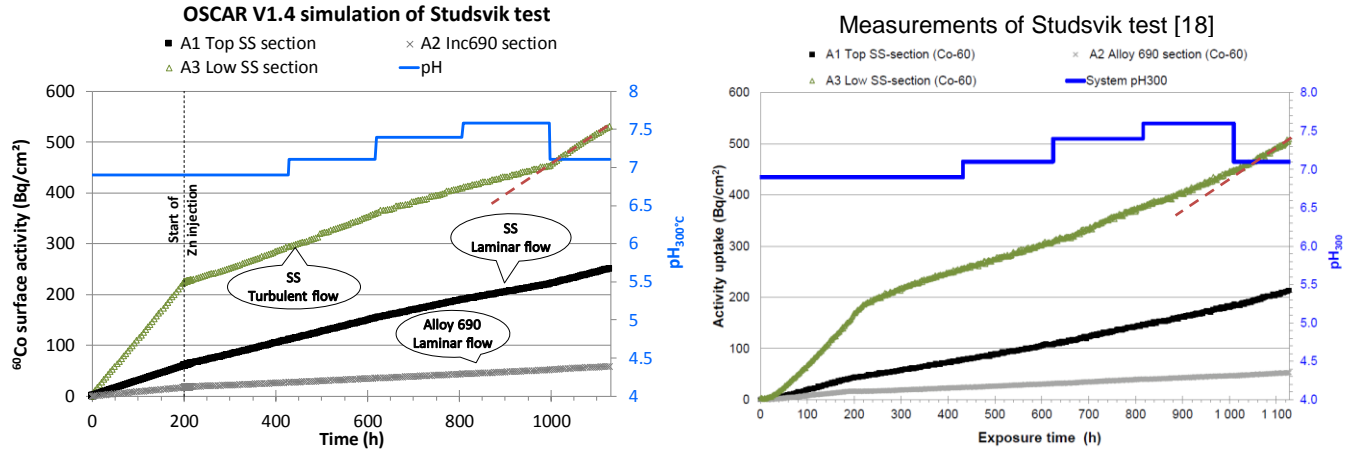


Figure 3: OSCAR V1.4 results (left) / Studsvik measurements (right [18]) –  $^{60}\text{Co}$  activity uptake. Effect of material, flow regime, Zn and pH.

### Simulation of a typical PWR

The simulated PWR is a French 900 MWe PWR equipped with Inconel 600 SG tubes (Co content of 300 ppm). The RCS and CVCS are described by 78 regions including 42 for the core (see Fig. 4). The first 20 cycles are simulated and each cycle lasts 282 days with a shutdown of 25 days (shutdown of 75 days at cycle 10). The simulated chemistry is a coordinated B-Li chemistry at aimed  $\text{pH}_{300^\circ\text{C}}$  of 7.2 and the hydrogen concentration is 30 mL/kg. The operating parameters are presented in Fig. 5 (cold shutdown parameters shown at cycles 1, 10 and 20). One-third of the fuel elements is replaced by fresh ones at the end of each cycle. From the 5<sup>th</sup> cycle, the fuel assembly grids made of 718 alloy are replaced by Zircaloy grids. The CVCS purification flowrate is 22 t/h with a purification efficiency of 99%.

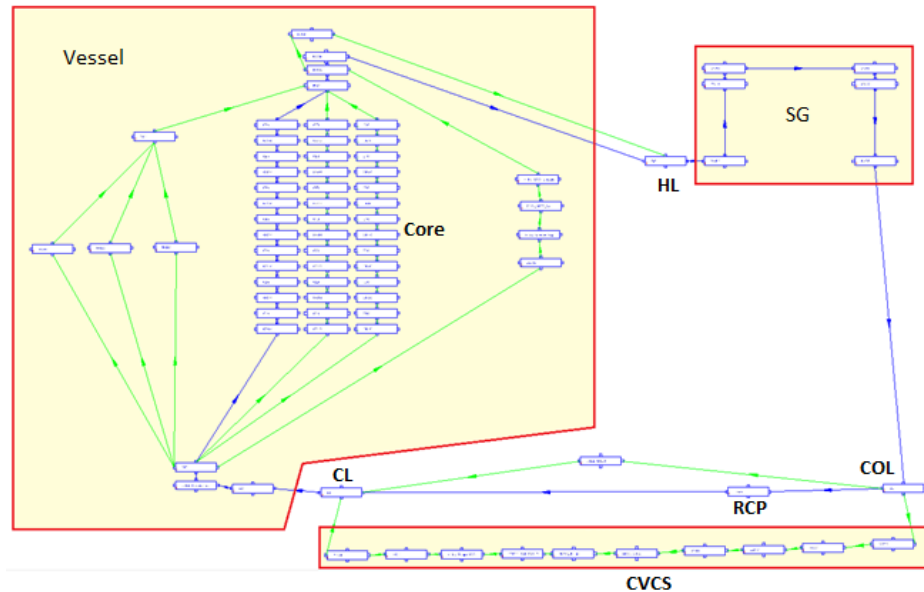


Figure 4: OSCAR V1.4 – Control volumes of the typical PWR (HL: Hot Leg / SG: Steam Generator / COL: CrossOver Leg / RCP: Reactor Coolant Pump / CL: Cold Leg).

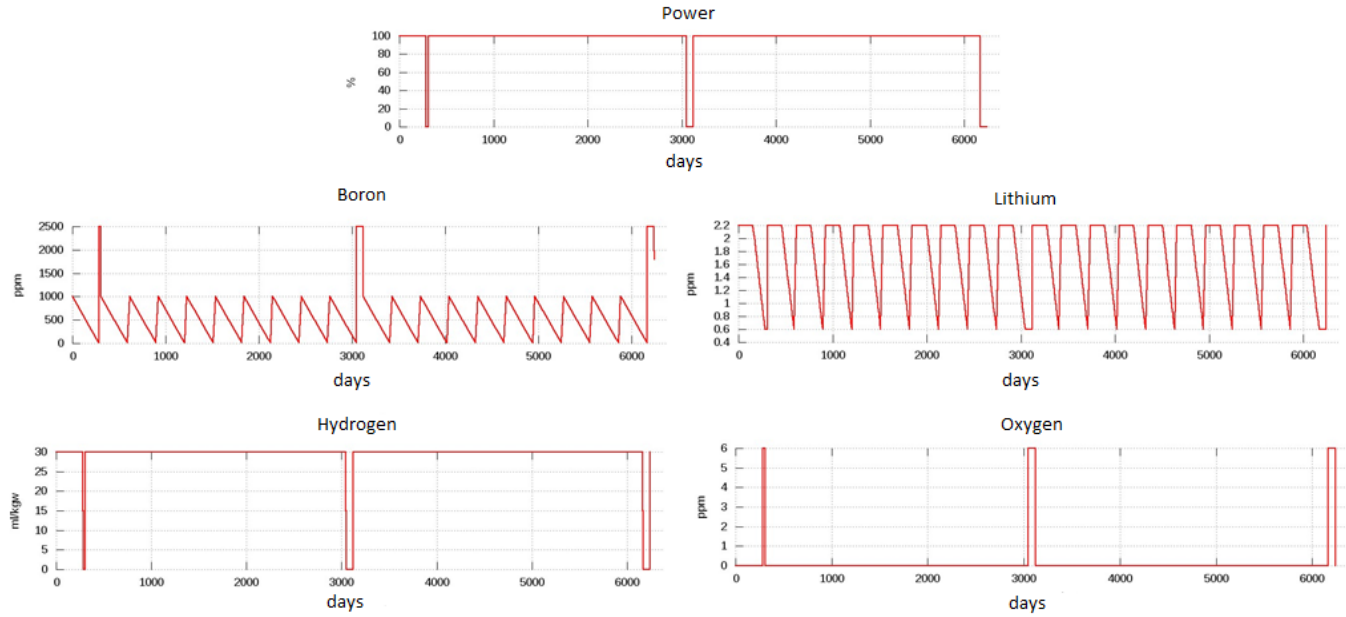


Figure 5: OSCAR V1.4 – Simulated operating parameters of the typical PWR.

**Surface activities.** To illustrate the capacity of the OSCAR V1.4 code to calculate the surface activities, Fig. 6 compares OSCAR V1.4 results on the typical PWR with EMECC measurements on the French fleet of 900 and 1300 MWe PWRs. The  $^{58}\text{Co}$  (activation product of Ni),  $^{60}\text{Co}$  (activation product of Co), and  $^{54}\text{Mn}$  (activation product of Fe) surface activities on the hot legs and on the cold side of steam generator tubes are presented in Fig. 6. The OSCAR code correctly calculates the right levels of the surface activities of the PWR primary systems. The calculated surface activities of the typical PWR are within the range of the measured surface activities of the French PWRs.



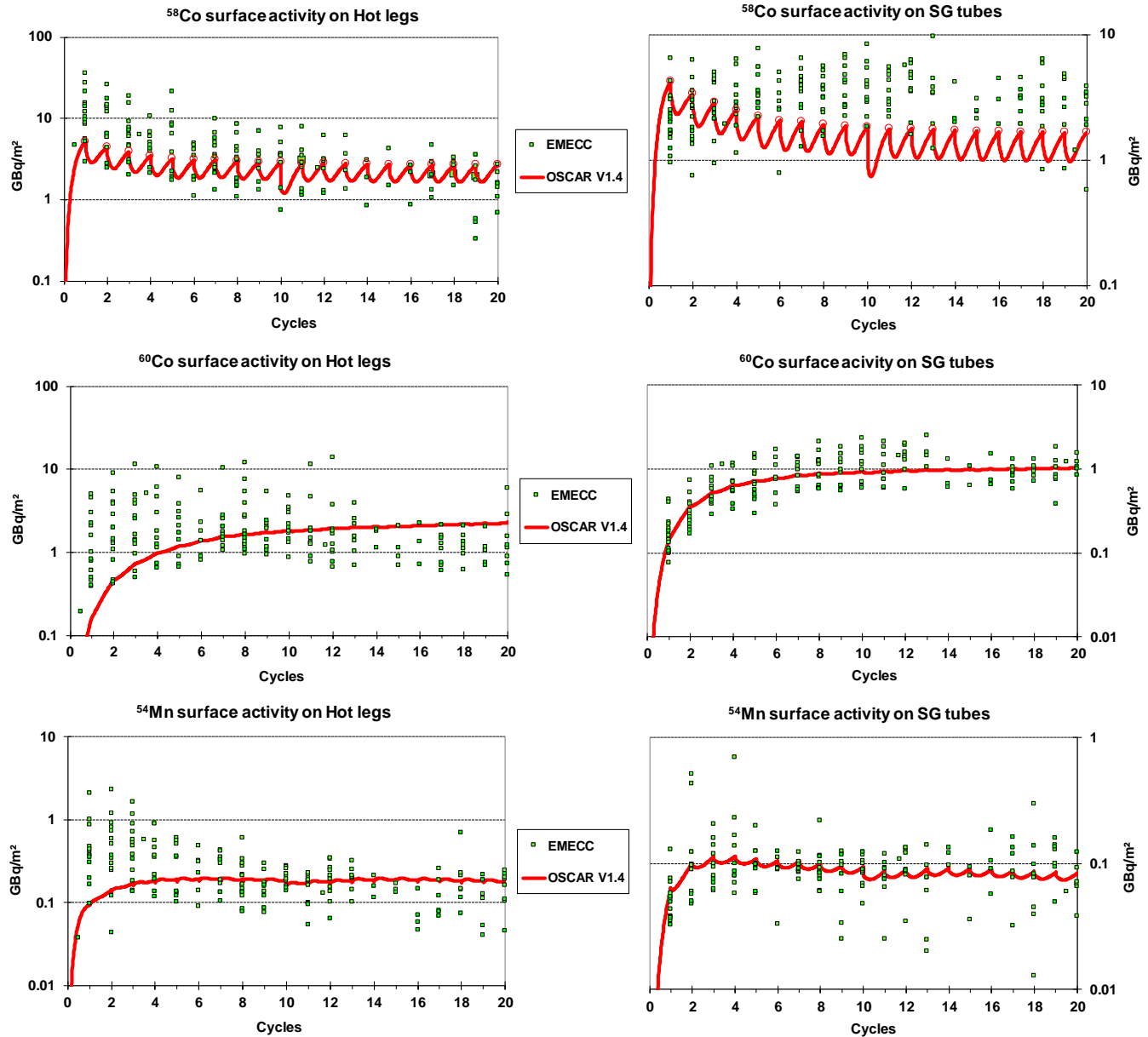


Figure 6: Comparison OSCAR V1.4 / EMECC measurements –  $^{58}\text{Co}$ ,  $^{60}\text{Co}$  and  $^{54}\text{Mn}$  surface activities on the hot legs and on the SG tubes – Red line: OSCAR V1.4 simulation of the typical PWR / Green squares: EMECC measurements of the French units (at the end of each cycle, a green square is a PWR case).

**Volume activities.** Fig. 7 presents the  $^{58}\text{Co}$ ,  $^{60}\text{Co}$ ,  $^{54}\text{Mn}$  and  $^{51}\text{Cr}$  volume activities of the typical PWR calculated using OSCAR V1.4.

The calculated volume activities are within the range of the measured volume activities of French PWRs: about 10 MBq/t for  $^{58}\text{Co}$ , about 1 MBq/t for  $^{60}\text{Co}$ ,  $^{54}\text{Mn}$  and  $^{51}\text{Cr}$ .

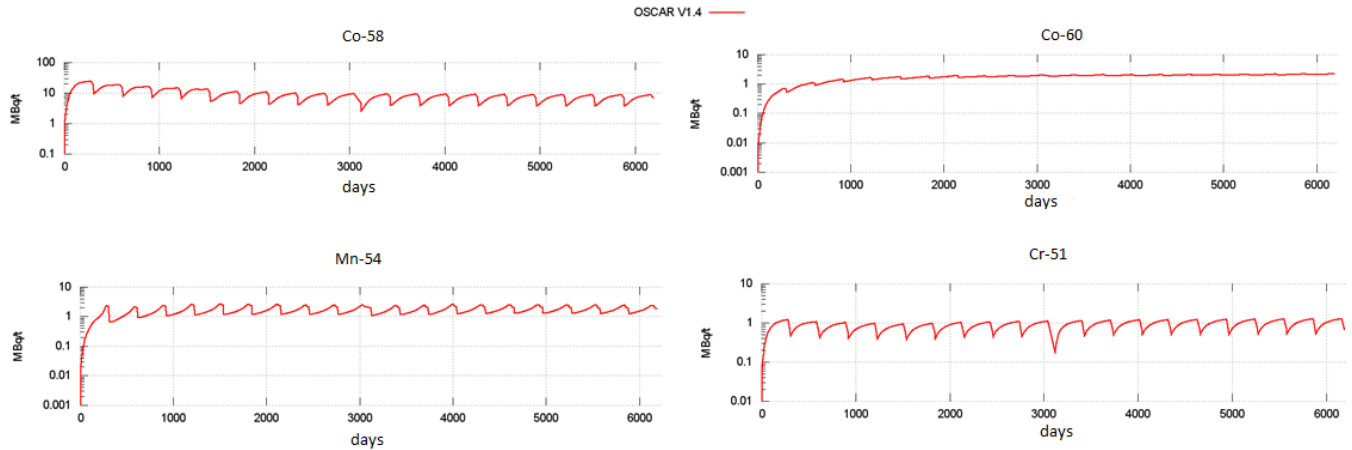


Figure 7: OSCAR V1.4 – Calculated  $^{58}\text{Co}$ ,  $^{60}\text{Co}$ ,  $^{54}\text{Mn}$  and  $^{51}\text{Cr}$  volume activities of the primary coolant of the typical PWR.

**Element concentrations.** The concentrations of Ni, Fe and Co calculated using OSCAR V1.4 are presented in Fig. 8.

The calculated concentrations are close to the typical concentrations measured in EDF PWRs: 1-2 ppb for Ni, about 1 ppb for Fe and 2 ppt for Co.

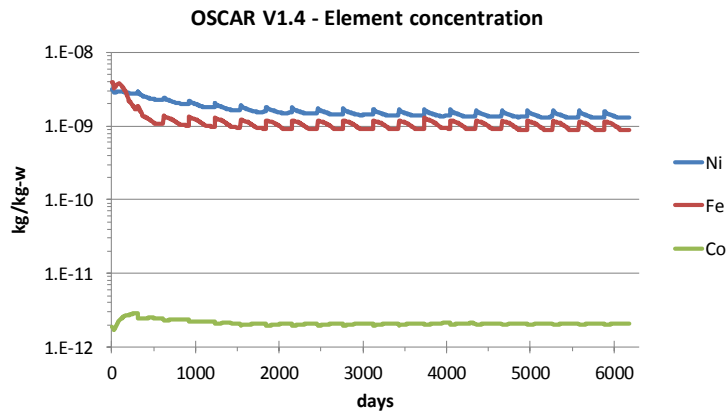


Figure 8: OSCAR V1.4 – Calculated concentrations of Ni, Fe and Co of the primary coolant of the typical PWR.

**Simulation of a cold shutdown.** Physico-chemical conditions significantly vary during a cold shutdown [20]: decrease in power, in temperature and in pH, oxygenation of the primary coolant. These changes lead to a release of corrosion products into the primary coolant. The RCS oxygenation causes a large dissolution of the in-core  $\text{Ni}^\circ$  deposit. The  $\text{Ni}^\circ$  deposit dissolution involves the dissolution of  $^{58}\text{Co}$  coming from the neutron activation of  $^{58}\text{Ni}$ .  $\text{Ni}^\circ$  peak concentration and  $^{58}\text{Co}$  peak activity then appear, typically, of the order of several ppm and 100 GBq/t, respectively [20] (except for PWRs equipped with improved manufacturing process SG tubes [21]).

To simulate these releases, it is necessary:

- To know the solid speciation of the crud on fuel elements (determined by OSCAR/PHREEQCEA) ;
- To vary the dissolution surface reaction rate of each phase ( $V_{dissol}^{phase_n(elt)}$ , see section Dissolution-Precipitation) as a function of temperature, pH and hydrogen/oxygen partial pressures ;
- To increase the dissolution rate of  $\text{Ni}^\circ$  in oxidizing conditions by means of the increase in the dissolution surface reaction rate of phase  $\text{Ni}^\circ$  ;

- To link the dissolution of  $^{58}\text{Co}$  coming from the Ni activation to the dissolution of  $\text{Ni}^\circ$  deposited on the fuel elements.

The coolant temperature, the CVCS flowrate, the boron, dihydrogen and dioxygen concentrations during a typical cold shutdown procedure are presented in Fig. 9. The calculated  $^{58}\text{Co}$  volume activity and  $^{58}\text{Co}$  specific activity during the cold shutdown of cycle 1 of the typical PWR is presented in Fig. 9 as well.

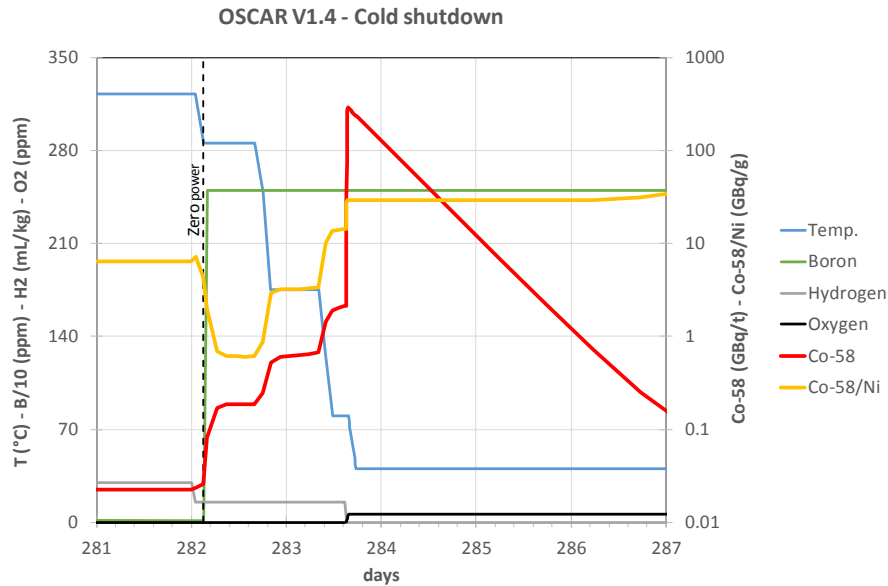


Figure 9: OSCAR V1.4 – Simulation of a cold shutdown procedure.

The changes and the levels of the  $^{58}\text{Co}$  volume activity are well reproduced [20]. The boron increase and the temperature drop lead to an increase in the volume activities considering that the ion equilibrium concentrations of corrosion products are higher at lower temperature and pH, and, on the other hand, the dissolution surface reaction rates of phases are higher at a lower pH. This increase is mainly due to the ferrite dissolution of the out-of-core and in-core deposits ( $^{58}\text{Co}$  specific activity below about 10), whereas the oxygenation mainly causes the in-core  $\text{Ni}^\circ$  deposits and thus in-core  $^{58}\text{Co}$  to dissolve quickly ( $^{58}\text{Co}$  specific activity of about 30). The calculated  $^{58}\text{Co}$  peak activity is about 350 GBq/t, which is within the range of the measured peak volume activities of the French PWRs at cycle 1. The decrease after the peak activity is due to the purification by the CVCS.

The cold shutdowns of the first 10 cycles and of cycle 20 have also been simulated<sup>3</sup>, the  $^{58}\text{Co}$  peak volume activities are presented in Fig. 10. The calculated  $^{58}\text{Co}$  peak activity decreases during the first 10 cycles from about 350 GBq/t to 120 GBq/t and stabilizes. These levels and variations are consistent with the French operational experience feedback.

<sup>3</sup> The  $^{58}\text{Co}$  peak activities at cycles 11 to 19 are not calculated but the effects of the cold shutdowns at cycles 11 to 19 are taken into account in the OSCAR calculation.

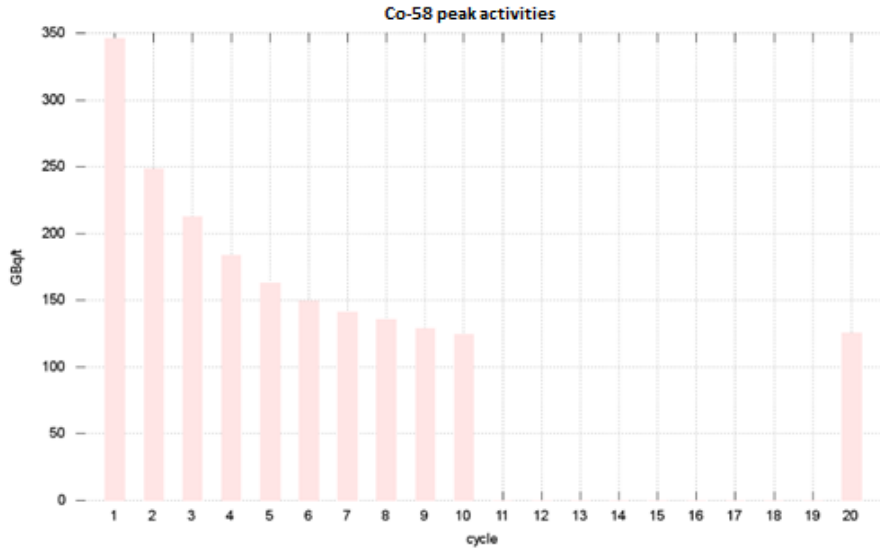


Figure 10. OSCAR V1.4 – Calculated  $^{58}\text{Co}$  peak volume activity of a typical cold shutdown procedure at the end of cycles 1 to 10 and 20.

## Conclusion

For more than 40 years, CEA has developed a code to calculate the contamination transfer in the nuclear systems: the OSCAR code. In the last version, OSCAR V1.4, the dissolution-precipitation model has been improved:

- The expressions of the dissolution and precipitation mechanisms are the same (the precipitation rate is a function of the dissolution velocity) ;
- The dissolution velocity depends on temperature, pH,  $p_{\text{H}_2}$  and  $p_{\text{O}_2}$ ;
- The new way to consider an isotope of an element enables the precipitation of this isotope even under unsaturated conditions of the element.

Thanks to this improvement and to the OSCAR chemistry module, PHREEQCEA, the OSCAR V1.4 code can reproduce the impact of pH, of Zn injection and of flow regime on the  $^{60}\text{Co}$  contamination of stainless steel and alloy 690 highlighted in an experiment performed by Studsvik. This improvement also allows us to better simulate the behavior of corrosion products due to the decrease in pH during a cold shutdown procedure.

The contamination levels of the PWR primary circuit and auxiliary systems as well are within the range of the operational experience feedback.

This new version of the OSCAR code is a powerful tool to analyze the behaviors of corrosion products in different conditions and thus to give explanations on these behaviors, e.g. [22].

## Acknowledgements

The authors are thankful to J. Öijerholm from Studsvik Nuclear AB for provided information on the Studsvik experiment simulated using OSCAR V1.4.

## References

1. P. Beslu and C. Leuthrot, “PACTOLE-PROFIP: two codes allowing prediction of the contamination of PWR primary circuits”, *Revue Générale Nucléaire*, November-December 1990, p552-554, 1990.
2. J.B. Genin, H. Marteau, F. Dacquait, G. Bénier, J. Francescato, F. Broutin, F. Nguyen, M. Girard, L. Noirot, S. Maillard, V. Marelle, A. Bouloré, D. You, G. Plancque, G. Ranchoux, J. Bonnefon, V. Bonelli, M. Bachet, G. Riot and F. Grangeon, “The OSCAR code package: a unique tool for simulating PWR contamination”,

- Proceeding of the International Conference on Water Chemistry of Nuclear Reactors Systems, NPC, October 2010, Quebec (Canada), 2010.
3. F. Dacquait, J. Francescato, F. Broutin, J.B. Genin, G. Bénier, M. Girard, D. You, G. Ranchoux, J. Bonnefon, M. Bachet and G. Riot, "*Simulations of corrosion product transfer with the OSCAR V1.2 code*", Proceedings of the international conference on Water chemistry in nuclear reactors systems, 24-28/09/12, Paris (France), Paper 193, 2012.
  4. F. Dacquait, *to be published*.
  5. D. L. Parkhurst and C. A. J. Appelo, "*Description of Input and Examples for PHREEQC Version 3 - A Computer Program for Speciation, Batch-Reaction, One-Dimensional Transport, and Inverse Geochemical Calculations*", US Geological Survey, Denver, Colorado, 2013.
  6. G. Plancque, D. You, E. Blanchard, V. Mertens and C. Lamouroux, "*Role of chemistry in the phenomena occurring in nuclear power plants circuits*", Proceedings of the International Congress on Advances in Nuclear power Plants, ICAPP, 2-5 May 2011, Nice (France), 2011.
  7. G. Plancque, D. You, V. Mertens and E. Blanchard, "*Experimental study and modeling of the corrosion product dissolution. Applications to PWR conditions (nominal operating and cold shutdowns conditions)*", Proceedings of the International Conference on Water Chemistry of Nuclear Reactors Systems, October 2008, Berlin (Germany), 2008.
  8. J. W. Cleaver and B. Yates, "*Mechanism of Detachment of Colloidal Particles from a Flat Substrat in a turbulent Flow*", Journal of Colloid and Interface Science 44, vol 3, 1972.
  9. S.K Beal, "*Deposition of particles in turbulent flow on channel or pipe walls*", Nuclear science and engineering, vol. 40, p.1-11, 1970.
  10. S.J. Michell, "*Fluid and particle mechanics*", Pergamon press Ltd, 1970.
  11. A.C. Ponting and R.S. Rodlife, "*Intrinsic filtration and retarded deposition for the control of colloidal corrosion product deposition on PWR fuel*", Water chemistry of nuclear reactor system, Proceedings of the BNES, 1983, p. 43-51, Bournemouth UK, 1983.
  12. A. Ferrer, "*Modélisation des mécanismes de formation sous ébullition locale des dépôts sur les gaines de combustible des Réacteurs à Eau sous Pression conduisant à des activités volumiques importantes*", PhD thesis, Université de Strasbourg, 2013.
  13. D. You *et al.*, CEA internal report, 2016.
  14. M. Girard, J.B. Genin, F. Dacquait, G. Ranchoux and G. Riot, "*Experimental study of particle deposition kinetics in the primary circuit of the CIRENE loop and comparison with OSCAR V1.2 code simulations*", Proceedings of the international conference on Water chemistry in nuclear reactors systems, 24-28/09/12, Paris (France), 2012.
  15. F. Dacquait *et al.*, CEA internal report, 2017.
  16. F. Dacquait, C. Andrieu, L. Guinard, J.L. Bretelle, F. Bardet, A. Rocher and C. Brun, "*Status of primary system contamination in French PWRs*", Proceedings of the international conference on Water chemistry in nuclear reactors systems, 11-14/10/04, San Francisco (US), Session 2 Paper 4, 2004.
  17. R. Eimecke and S. Anthoni, "*Ensemble de Mesure et d'Etude de la Contamination des Circuits (EMECC)*", 7th International Conference on Radiation Shielding, 12-15 September 1988, Bournemouth (England), 1988.

18. J. Öijerholm, B. Bengtsson, P. Gillén and P. Svanberg, "*Influence of pH, Temperature and Flow Velocity on Co-60 Uptake on Alloy 690 and Stainless Steel in Simulated PWR Chemistry*", Proceedings of the international conference on water chemistry in nuclear reactors systems, NPC 2016, 2-7/10/16, Brighton (GB), Paper 52, 2016.
19. F. Dacquait *et al.*, *to be published*.
20. F. Dacquait, C. Andrieu, M. Berger, J.L. Bretelle and A. Rocher, "*Corrosion product transfer in French PWRs during shutdown*", Proceedings of the International conference on water chemistry in nuclear reactors systems, 22-26/04/02, Avignon (France), CD-ROM, paper 113, 2002.
21. F. Dacquait, L. Guinard, F. Bardet, J. L. Bretelle and A. Rocher, "*Low Primary System Contamination Levels in Some French PWRs*", Proceedings of the International conference on water chemistry in nuclear reactors systems, 23-26/10/06, Jeju Island (Korea) paper 2.17, 2006.
22. T. Jobert, C. Cherpin, F. Dacquait, J-B. Genin and E. Tevissen, "*Impact of the B/Li coordinated chemistries on the surface contamination of a French PWR using the OSCAR V1.4 code*", this conference.